Hip and Trunk Kinematics Estimation in Gait Through Kalman Filter Using IMU Data at the Ankle

Amir Baghdadi, Lora A. Cavuoto, and John L. Crassidis

***Abstract*— The purpose of this paper is to provide a new method of estimating the hip acceleration and trunk posture in the sagittal plane during a walking task using an extended Kalman filter (EKF) and an unscented Kalman filter (UKF). A comparison between these two estimation techniques is also provided. Considering the periodic nature of gait, a modified biomechanical model with Fourier series approximations are utilized as *a priori* knowledge. Inertial measurement units (IMUs) are placed on the right side of the ankle, hip, and middle of the trunk of twenty recruited participants, as input, *a posteriori* data, and the ground truth for the model, separately. The results show a better performance of the EKF in estimating the hip acceleration (6.5% error) and the trunk posture (3.12% error). Moreover, both the EKF and the UKF provide low error rates for the trunk posture in comparison to the hip acceleration. This paper provides an inexpensive and novel method to estimate and filter the kinematics of motion for different body locations from a single accurate IMU attached to the ankle considering the periodic nature of gait that can be extended to other activities as well as real-time applications.**

***Index Terms*— Gait kinematics, biomechanical model, inertial measurement unit, Kalman filter, kinematics estimation.**

I. Introduction

KNOWING the upper body kinematics is necessary for a broad range of applications in clinical evaluation and decision making for patients with upper extremity disorders [1], including monitoring and analysing patient movements in the process of rehabilitation [2], spine and shoulder girdle movements analysis during gait for patients with idiopathic scoliosis [3], and gait movement evaluation for children with cerebral palsy [4]. In addition, stability and energy efficiency analysis of walking using upper body kinematics has been a topic of study [5], [6], which highlights the importance of its monitoring and estimation.

In worker safety, evaluating the upper body kinematcis can be used for the purpose of postural stability analysis to reduce the rate of falls risk [7], as well as identifying static neck and shoulder posture to avoid the risk of neck and upper limb disorders in office workers [8]. In order to obtain postural information along with other safety purposes, monitoring of workers has been considered. Examples include real-time posture analysis using a camera [9] for ergonomics training to prevent fatigue, and sensor-based observation of personnel location and activity for safety and performance evaluation goals [10]–[12].

Sensor systems including wearable movement and physiological measurement devices have become prominent in human activity and physical monitoring due to their affordability, convenience, and minimal intrusiveness. In safety surveillance, these applications range from fall detection [13] and posture analysis [14], to task classification [15] and fatigue detection [16], [17]. Studies have been conducted for estimating the lower limb kinematics in the sagittal plane by fusing the data of two accelerometers and gyroscopes placed on the ankle and shank [18] or the lower back [19] by means of a customized fusion technique and Fourier linear combiner, respectively. However, these applications require using multiple sensors on the body. For field-based applications, it is desirable to use a smaller number and simpler set of sensors on non-intrusive body locations, and estimate the kinematics of other target locations using estimation techniques instead of direct measurement.

The kinematics estimation of upper body has limitations, in comparison to the lower body, on the performance of the methods and results. The importance of trunk kinematics estimation has been addressed in the literature for assessing the spatio-temporal gait parameters as well as lower limb and spine moments [20]–[22]. Additionally, hip and trunk kinematics are useful for the purpose of human fatigue detection [23], [24]. The upper extremity has rapid, complex, and less periodic pattern that hinders the use of measurement devices, e.g. marker system or IMUs [25], which highlights the importance of estimation for kinematics in those locations from more feasible locations in terms of sensor placement.

The Kalman filter, a well-known estimation technique, has proven efficient in many applications [26]. This technique improves the estimation of a desired variable by incorporating measurements from other sources and predictions from the physical model, which is more precise than only the measurement outcomes. There are two options for Kalman estimation in non-linear physical models including

Manuscript received December 13, 2017; revised March 14, 2018; accepted March 14, 2018. Date of publication March 19, 2018; date of current version April 23, 2018. This work was supported by the American Society of Safety Engineers Foundation through the grant Advancing Safety Surveillance using Individualized Sensor Technology. The associate editor coordinating the review of this paper and approving it for publication was Prof. Aime Lay-Ekuakille. *(Corresponding author: Lora A. Cavuoto.)*

A. Baghdadi and J. L. Crassidis are with the Department of Mechanical and Aerospace Engineering, University at Buffalo, State University of New York, Buffalo, NY 14260 USA.

L. A. Cavuoto is with the Department of Industrial and Systems Engineering, University at Buffalo, State University of New York, Buffalo, NY 14260 USA (e-mail: loracavu@buffalo.edu).

Digital Object Identifier 10.1109/JSEN.2018.2817228

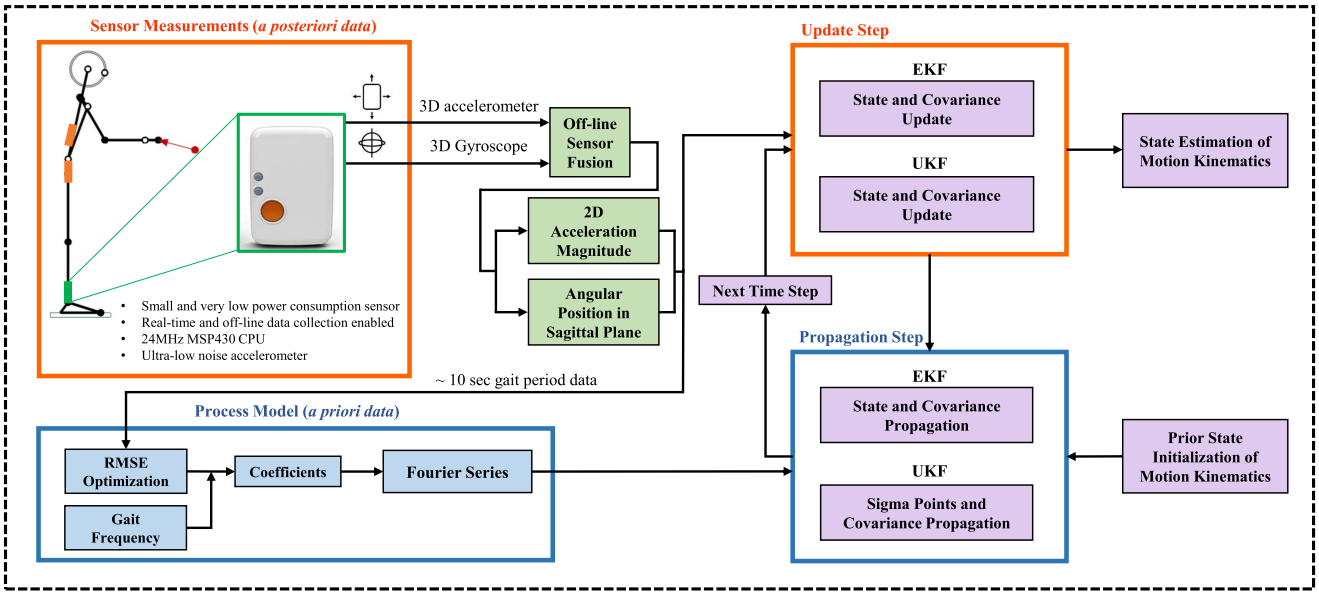

Fig. 1. Diagram of sensor system within the Kalman Filter algorithm.

the Extended Kalman filter (EKF) and its subsequent improved version, unscented Kalman filter (UKF). The former linearizes the equations about an estimate of mean and covariance for the working point, and the latter uses a minimum number of sample points around the mean value using a deterministic sampling technique and propagates them through the highly non-linear model function to estimate the new mean and covariance points. This technique removes the calculation of Jacobians that can be burdensome in many complex model functions. These Kalman filters, as two alternatives for non-linear physical models, have been compared in navigation systems [27], however there are limited application of these filters in human body kinematics estimation.

The main purpose of this paper is to estimate and track the motion in different locations of the human body in real-time, given the kinematics of motion from an IMU attached to the ankle, and to compare the performance of the Extended Kalman Filter (EKF) and Unscented Kalman Filter (UKF). The use of nonlinear Kalman filters is considered here since the biomechanical modeling of human gait ends up in a nonlinear dynamic system. In addition, the utilization of the Kalman filter was examined for filtering the motion parameters and providing an estimated result that maintains the main characteristics of the original data obtained from an independent accurate measurement sensor attached to the target locations. In this case, we aim to estimate and filter the acceleration at the hip joint and posture of the trunk in the sagittal plane during gait.

II. Methods

A. Sensor System and Data Processing

The sensor system consisted of one IMU attached at each of the right ankle, right side of the hip, and middle of the trunk locations. The sensor at the ankle serves as the input for the estimation method, while the other two are used as the ground truth for performance evaluation purpose. The sensors used here are Shimmer3 IMUs (Shimmer3, SHIMMER, Dublin, Ireland, www.shimmersensing.com), which have been previously used for wearable and remote applications in the areas of monitoring human health and tracking activities of daily living [28]–[30]. These sensors consist of a low noise 3-axis accelerometer with $\pm$ 2g range and RMS noise of $5.09 \times 10^{-3} \mathrm{m/s^2}$ as well as the gyroscope with $\pm$ 2000 dps range and RMS noise of 0.0481 dps. The sensors are small (51mm $\times$ 34mm $\times$ 14mm), lightweight (23.6 grams), fully portable, and easily attachable with designated straps. The sensor system is provided in the Sensor Measurements section of Fig. 1. The employment of sensor systems for gait analysis has been studied before, however, using different sensing devices and for different applications. In one study, the estimation accuracy of pelvis and hip kinematics is shown to be necessary in improving the calculation errors for the angles in other joints defining the human movement [31]. In addition, the accuracy of measurements is documented to be crucial in providing a reliable foundation for gait analysis with various applications that range from gait biometrics for security purposes to movement monitoring in athletes, highlighting the importance of a proper design and architecture for the sensing and estimation system [32]–[35].

The low noise 2D (x-y axes) acceleration and rotational velocity from the gyroscope were used after an off-line sensor fusion technique described in [16]. The sensor data was used for the following purposes: 1) optimization of the Fourier series coefficients, 2) input measurement data to the Kalman filter, and 3) ground truth for the evaluation of the kinematic estimations. As shown in the data processing algorithm laid out in Fig. 1, the Kalman filter consisted of two major steps: 1) updating the state estimate of motion kinematics by comparing against the *a posteriori* data from the sensor

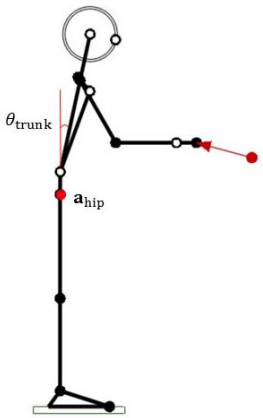

Fig. 2. Biomechanical model diagram. Angular position θ_{trunk} is defined relative to the vertical axis in the sagittal plane, counter-clockwise being positive. $\mathbf{a}_{\text{hip}}$ is the acceleration magnitude at hip joint. The figure is generated using University of Michigan 3D Static Strength Prediction Program (3DSSPP) Software.

measurement and 2) prediction of the kinematics state estimate using the *a priori* information from the biomechanical process model.

B. Biomechanical Process Model

In order to estimate the kinematics of motion as the system state, a process model (i.e. *a priori* knowledge) is required to represent the dynamics of the human musculoskeletal system [36]. However, the complexity of dynamic models for the human musculoskeletal system, which has been well studied during the past years [36], hinders the application of estimation algorithms, i.e. Kalman filtering, due to large algebraic equations obtained by the derivatives of the original position model (e.g. acceleration or jerk). To suppress this problem, the kinematics of the hip and trunk is modeled as a function of ankle kinematics due to the periodic nature of gait:

$$x_{\text{hip}} = f(x_{\text{ankle}}) \tag{1a}$$

$$\theta_{\text{trunk}} = f(\theta_{\text{leg}}). \tag{1b}$$

This idea has also been used in [37] to obtain the ankle displacement from foot rotation. This multi-segment model (Fig. 2) is considered as *a priori* information to relate the kinematics of the ankle to the hip and trunk.

By taking the derivative of Equation (1a), the hip acceleration can be related to the ankle kinematics:

$$\ddot{x}_{\text{hip}} = \frac{d^2 f}{dx_{\text{ankle}}^2}\dot{x}_{\text{ankle}}^2 + \frac{df}{dx_{\text{ankle}}}\ddot{x}_{\text{ankle}}. \tag{2}$$

It is assumed that, during the gait cycle, at least one foot is in contact with the ground so that the position of the other joint centers in the model can be derived from the ankle joint position. By considering the cyclic nature of gait, the joints' angular and linear kinematics can be represented as a Fourier series [37]:

$$g(t) = a_0^{(i)} + \sum_{k=1}^{n}(a_k^{(i)}\cos(k\omega t) + b_k^{(i)}\sin(k\omega t)), \tag{3}$$

where n is the order of the Fourier series and $\omega = 2\pi/T_c$ is the walking frequency such that T_c is the walking period.

The experimental data of gait kinematics from the IMUs attached to the ankle, hip, and trunk during a $\sim$ 10 sec gait period is used to calculate the coefficients of the Fourier series, i.e. $a_0^{(i)}$, $a_k^{(i)}$, and $b_k^{(i)}$. They are found through minimizing the root-mean-square error (RMSE) between experimental data and the process model. Equations (4a) to (4d) show the results for a 29-year old female subject with 177 cm stature and 70.2 kg body mass. The Fourier series are used as the model for the hip and ankle linear accelerations as well as the leg and trunk angular positions, as follows:

$$\mathbf{a}_{\text{hip}} = 3.13(3.22 + \sum_{k=1}^{4}(\cos(16.25kt) - \sin(16.25kt))) \tag{4a}$$

$$\mathbf{a}_{\text{ankle}} = 3.21(2.85 + \sum_{k=1}^{3}(\cos(6.15kt) - \sin(6.15kt))) \tag{4b}$$

$$\theta_{\text{leg}} = 13(0.3 + \cos(5.95(t+0.75)) + \sin(5.95(t+0.75))) \tag{4c}$$

$$\theta_{\text{trunk}} = 5(-0.5 + \cos(6.15(t-0.75)) + \sin(6.15(t-0.75))). \tag{4d}$$

Having the process model, *a priori* information can be provided for the Kalman filter in order to propagate the state variables. Due to nonlinearity of the process model, Equations (4a) to (4d), the nonlinear versions of the Kalman filter, i.e. EKF and UKF, are used. For the next step, since the measurement and process models are discrete and continuous, respectively, continuous-descrete Kalman filters are employed with the same update and propagation steps as the linear Kalman filter.

C. Extended Kalman Filter

The first choice of estimator is the EKF that linearizes the nonlinear process model about the estimate of the current mean and covariance. A small error is assumed for the kinematic parameters in the state vector so that they can be approximated using a first-order truncated Taylor series expansion. The tracker state vector of the filter contains trunk and ankle angular posture as well as hip joint and ankle acceleration, which is defined as,

$$\mathbf{x} = [\mathbf{a}_{\text{hip}}, \theta_{\text{trunk}}, \mathbf{a}_{\text{ankle}}, \theta_{\text{leg}}]^{\mathsf{T}}, \tag{5}$$

where $\mathbf{a}$ is the acceleration and θ is the angular position relative to the vertical axis in sagittal plane as shown in Fig. 2. This approach of defining the tracker state vector has also been used in [38]. Using an accurate IMU attached to the ankle joint, the acceleration of the ankle and angular position of the leg are assumed to be available, so the measurement model is considered as

$$\mathbf{h} = [\tilde{\mathbf{a}}_{\text{hip}}, \tilde{\theta}_{\text{trunk}}]^{\mathsf{T}}. \tag{6}$$

The continuous time process model equations and discrete time measurements acquired from the sensors lead us to use a continuous-discrete Extended Kalman filter. More details about the filter can be found in [26]. The model formulation

using Equations (4a) to (4d) in order to be used in the EKF can be written as

$$\dot{\mathbf{x}}(t) = \mathbf{f}(\mathbf{x}(t), t) + G(t)\mathbf{w}(t), \quad \mathbf{w}(t) \sim \mathcal{N}(0, Q(t)) \tag{7a}$$

$$\tilde{\mathbf{y}}_k = \mathbf{h}(\mathbf{x}_k) + \mathbf{v}_k, \quad \mathbf{v}(t) \sim \mathcal{N}(0, R_k), \tag{7b}$$

where $\mathbf{f}(\mathbf{x}(t), t)$ is a continuous function and also differentiable and $G(t)$ is the process noise state model. Furthermore, the state vector $\mathbf{x}$ and the measurement model $\mathbf{h}$ are defined in Equations (5) and (6) respectively. The terms $\mathbf{v}(t)$ and $\mathbf{w}(t)$ are assumed to be zero mean uncorrelated white Gaussian measurement and process noises, respectively. In addition, $Q(t)$ and R_k are the spectral density and covariance, respectively, indicating the confidence in the process model and measurement data [39].

The observation model H_k that maps the true state space model into the observed space and the state transition model $F(t)$ can be calculated by finding the Jacobian matrix of $\mathbf{f}$ and $\mathbf{h}$ as shown below:

$$F(\hat{\mathbf{x}}(t), t) \equiv \frac{\partial \mathbf{f}}{\partial \mathbf{x}}|_{\hat{\mathbf{x}}(t)} = \frac{\frac{d}{dt}[\mathbf{f}(\mathbf{x}(t), t)]}{\frac{d}{dt}[\mathbf{x}(t)]}|_{\hat{\mathbf{x}}(t)} \tag{8}$$

$$H_k(\hat{\mathbf{x}}_k^-) \equiv \frac{\partial \mathbf{h}}{\partial \mathbf{x}}|_{\hat{\mathbf{x}}_k^-} = \begin{pmatrix} 1 & 0 & 0 & 0 \\ 0 & 1 & 0 & 0 \end{pmatrix}. \tag{9}$$

In our notation *a posteriori* quantity which is after measurement update is represented by $(\cdot)^+$, and similarly *a priori* quantity which is after prediction by $(\cdot)^-$. The derivation of $F(\hat{\mathbf{x}}(t), t)$ in (8) is found through the chain rule and is not shown here. It is noteworthy that the state transition model F is calculated in each step at the estimate point $\hat{\mathbf{x}}(t)$, and the observation model H_k is calculated at the *a priori* state estimate $\hat{\mathbf{x}}_k^-$.

P_0 and $P(t)$ are initial and continuous error covariances. P_k^+ and P_k^- are *a posteriori* and *a priori* error covariances, respectively. *Joseph stabilized* version of covariance update [26] is used to ensure the stability of the filter.

The estimation of movement kinematics in EKF is performed in two steps. First, the update step in which *a posteriori* state estimate $\hat{\mathbf{x}}_k^+$ is found by updating the *a priori* state estimate $\hat{\mathbf{x}}_k^-$ and the measurement data $\tilde{\mathbf{y}}_k$ from the inaccurate sensors with uncertainties, attached to the hip and trunk. Second, the propagation step in which the state estimate is predicted using the process model transition function $\mathbf{f}$. In summary, the propagation step predicts the estimation of movement kinematics using the physical process model without considering any observation, on the other hand, the update step refines this prediction using the observed data through measurement.

D. Unscented Kalman Filter

An EKF is applied to estimate the state vector due to the nonlinearity of the process model. However, because of linearization, the EKF suffers from instability in the case of insufficiently small time intervals. Furthermore, Jacobian matrix calculation can be elaborate depending on the complexity of the system [40], [41]. In order to overcome these limitations and improve the filter, the Unscented Kalman Filter is used to calculate the mean and covariance of a Gaussian distribution representing the state of the system using deterministic sample points, sigma points, for the estimation process [41], [42]. In the UKF, instead of finding the Jacobian matrix of the state system, sigma points are transformed using the Unscented Transformation (UT). More details of the UKF can be found in [42].

The variable $\lambda = \alpha^2(L + \kappa) - L$ is defined in the UKF for calculating the sigma points, in which α is the primary scaling parameter and shows spread of the sigma points with larger numbers associated with more distributed points. β is the secondary scaling parameter containing the prior distribution information. This factor in the optimal case for Gaussian distribution is equal to two. κ contains information about the higher moments of the distribution with the default value equal to zero [42].

In order to estimate and track the kinematics of movement expressed as the state vector $\mathbf{x}$, using the UKF algorithm, a number of deterministic sigma points are generated and propagated through the state transition function $\mathbf{f}$ defined in (7a). In the next step, the sigma points are transformed through the measurement model function $\mathbf{h}$ and the *a priori* measurement estimate $\hat{\mathbf{y}}_k^-$ are calculated. Lastly, the state estimate $\hat{\mathbf{x}}_k$ is found by updating the *a priori* state estimate $\hat{\mathbf{x}}_k^-$ using the noisy measurement data $\tilde{\mathbf{y}}_k$ from the sensors attached to the hip and trunk.

E. Experimental Procedure

Fifteen males and five females (mean (standard deviation) age 33 (16.3) years, mean stature 171.3 (7.2) cm, and mean body mass 72.2 (14.3) kg) without any self reported injuries or musculoskeletal disorders are recruited to participate in this study. Study protocols were approved by the University at Buffalo Institutional Review Board and all participants completed an informed consent procedure after being informed about the details of the experiment. The experimental task is part of a larger study on physical fatigue induced by manual material handling. More information about the experimental setup and tasks is available in [24] and [16]. The participants are asked to walk on a set path while pushing a 2-wheeled dolly for carrying and delivering a set of boxes based on an order sheet.

F. Filter Parameters and Validity Assessment

The participants are equipped with IMUs on different body locations of right ankle, right side of the hip, and middle of the trunk. For this study, a portion of data ($\sim$ 10 sec) at a rate of 51.2 Hz are extracted from the pure walking period of each participant at the start of the 3-hour task to be used in the EKF and UKF. The implementation parameters of the filters are shown in Table I, which are found based on either the characteristics of the IMUs, initial values of *a posteriori* data, or through experiment.

In order to assess the stability of the EKF, a Lyapunov condition is considered:

$$\mathcal{L}(t) = H^T(t)R^{-1}(t)H(t) + P^{-1}(t)G(t)Q(t)G^T(t)P^{-1}(t). \tag{10}$$

TABLE I
KALMAN FILTER PARAMETERS INITIALIZATION

	EKF	UKF
Sampling time for dynamic model discretization (Δt)	0.0195 sec	0.0195 sec
Initial measurement noise covariance diagonal matrix (R_k) with $\mathbf{a}_{\text{hip}}$ and θ_{trunk} error terms	0.05 m^2/s^4 and $(\sqrt{0.5}$ deg$)^2$	0.05 m^2/s^4 and $(\sqrt{0.5}$ deg$)^2$
Initial error covariance diagonal matrix (P_0^-) for all error terms	0.5 m/s^2 and deg	0.5 m/s^2 and deg
Initial state vector values for $\mathbf{a}_{\text{hip}}$, θ_{trunk}, $\mathbf{a}_{\text{ankle}}$, and θ_{leg}	12 m/s^2, 10 deg, 15 m/s^2, and –6 deg	12 m/s^2, 10 deg, 15 m/s^2, and –6 deg
Initial process model covariance diagonal matrix ($Q(0)$) with $\mathbf{a}_{\text{hip}}$, $\mathbf{a}_{\text{ankle}}$, θ_{trunk} and θ_{leg} error terms	0.3 and 0.1 m/s^2 and 0.5 and 0.2 deg	10 and 2 m/s^2 and 1.5 and 0.2 deg
UKF scaling parameters α, β, and κ	-	10^{-2}, 2, and zero

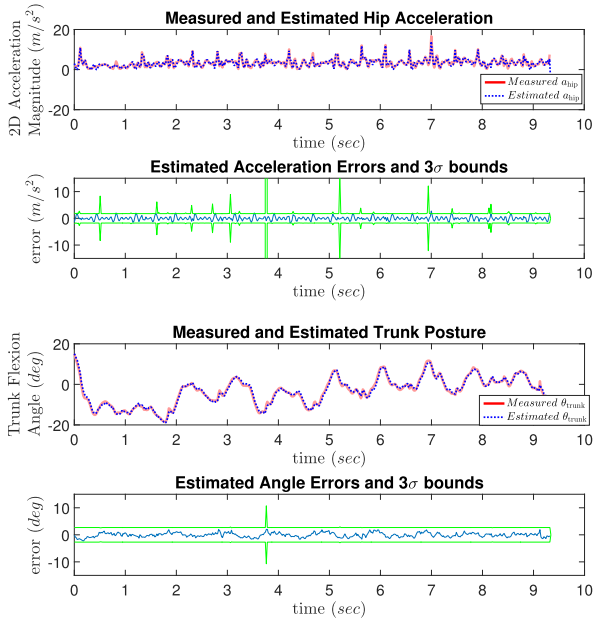

Fig. 3. Measured and estimated results of Extended Kalman Filter for participant number 3 who was a 27-year old male with 181 cm stature and 88.2 kg body mass.

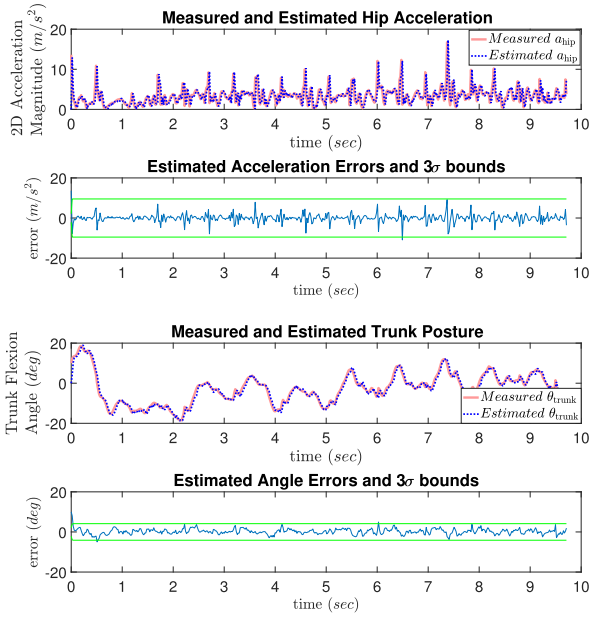

Fig. 4. Measured and estimated results of Unscented Kalman Filter for participant number 3 with the details provided in the caption for Fig. 3.

In addition, to provide a further validity assessment for the filter outcome, the discrete time covariance matrix defined in Square Root Information Filter (SRIF) presented by [26] was calculated for interpreting the fluctuations in the EKF.

III. RESULTS

The graphical results of hip acceleration and trunk posture estimation for one subject with comparison to the ground truth obtained from an accurate IMU attached to the target locations using EKF and UKF are provided in Fig. 3 and Fig. 4, respectively. The ground truth input data to the model and the measured values for that subject are provided separately in Fig. 5. The graphs show the convergence of error to their respective 3σ error bounds for both the EKF and UKF. The results presented in Table II indicate the better performance of the EKF in comparison to the UKF in terms of the mean (standard deviation) error rates for relative and absolute errors across all 20 participants. The results of Lyapunov condition for the EKF stability assessment showed that the $\mathcal{L}(t)$, $R(t)$, and $Q(t)$ matrices are always positive definite, so the Lyapunov condition is satisfied and the EKF local stability is proved, meaning that the filter is able to track even in case of unbounded measurements.

TABLE II
RELATIVE AND ABSOLUTE ERROR RATES PRESENTED AS MEAN (SD)

	Hip Acceleration		Trunk posture	
Error type	EKF	UKF	EKF	UKF
Relative	6.5 (1.42) %	13.02 (2.19) %	3.12 (0.56) %	5.3 (0.82) %
Absolute	0.96 (0.09) m/s^2	1.99 (0.46) m/s^2	0.68 (0.11) deg	1.16 (0.17) deg

For the UKF, the 3σ error bounds become steady, whereas there exist fluctuations for the EKF that is due to the non-linearity of the system. For interpreting the fluctuations in the EKF, the SRIF discrete time covariance matrix was also calculated. The estimated errors with 3σ bounds using discrete time covariance are provided in Fig. 6. The bounded errors in the graphs show the stability of the filter even without the exact truth provided to the filter.

The accelerometers usually contain bias which needs to be estimated and corrected, however, in this case, since the duration of measurements is small (i.e. less than 10 sec), the bias is not likely to appear. Therefore, bias estimation has not been considered.

IV. DISCUSSION

This study shows that the EKF outperfoms the UKF in estimating hip acceleration and trunk posture (Table II). Considering the cyclic nature of walking, a Fourier series has been considered for representing the kinematics of motion

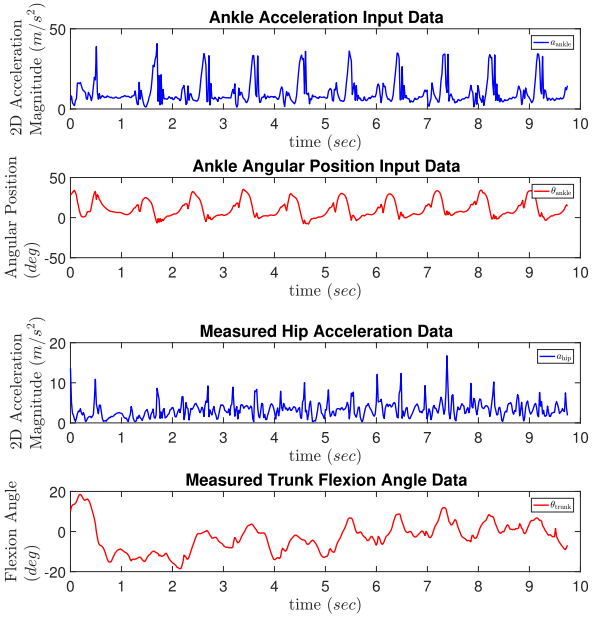

Fig. 5. Measured and input data of the model for participant number 3 with the details provided in the caption for Fig. 3.

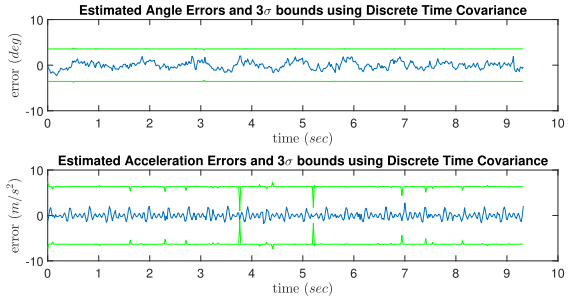

Fig. 6. Estimated errors of Extended Kalman Filter using SRIF discrete time covariance for participant number 3 with the details provided in the caption for Fig. 3.

where the coefficients have been derived by the minimization of the RMSE between experimental data and the process model. However, this poses uncertainties due to a rough approximation and can be associated to the lower accuracies in the estimation of hip acceleration for the UKF that shows a less periodic behavior when compared to the trunk posture. In addition, the anthropometric differences and various walking styles in the subjects can lead to a different biomechanical process model in the filter that can be another source of error for both acceleration and posture estimations.

The comparison of the UKF and EKF in [27] shows a slightly better performance for the UKF in the positioning module of an integrated navigation information system, however, they reported the inefficiency of the UKF in terms of computational time. The UKF employed here was additive noise due to the fluctuations in the sensor signal which is modelled heuristically with an additive zero mean uncorrelated white noise process in Equation (7b). In general, for certain highly non-linear systems, the more accurate performance of the UKF is expected since a minimal set of sample points are propagated through the non-linear function instead of the linearization approach used in EKF [27], [43], [44]. However, the UKF is proved to be sensitive for small variations in noise processes and the uncertainty of other parameters. In addition, the misalignment of covariance eigenvectors and high condition number of the matrices result in the misinterpretation of new residuals in the filter [45]. Reducing the uncertainties associated with the dynamic model estimated parameters by optimization methods for minimizing energy expenditure over a complete gait cycle [37] or Particle Swarm Optimization (PSO) to optimize the Fourier series parameters [46] will improve the performance of the filters.

To the best of our knowledge, acceleration estimation of different body locations studied here has not received much attention in the biomechanics literature, although it is an important metric considered for human fatigue analysis [24], [47]. For instance, [48] and [49] reported a post-fatigue decrease in the acceleration of lower back and center of body mass, respectively. Kinematics estimation of trunk posture has been studied using a single IMU placed on the lower back during squat exercise [19]. In that study, a weighted Fourier linear combiner was used to eliminate the drift associated with the position and angular calculations in the IMU data, then an inverse kinematic module computed the joint angles. Their results from human subject validation experiments showed the RMSE (SD) of 2.0 (1.5) deg for the torso angle in the sagittal plane. This method was limited to a quasi-periodic task of squat exercise and the main requisite of the biomechanical model was the fixed position of the foot. [18] estimated the lower limb orientation from IMUs attached to the centers of rotation using a new fusion technique that removes the drift in angular measurement calculations by the IMU attached to the target locations and showed the average RMSE of 1.0 deg and 1.6 deg in the shank and thigh, respectively. However, this was a new method in the kinematics estimation of an IMU rather than an extension of estimation to other body locations. The sagittal plane ankle, knee, and hip angles estimation from motion sensors on the foot and shank using generalised regression neural networks and training the model based on different gait styles from eight subjects by [50] also denoted an average error of 7.13 (1.92) deg. The limited number of training inputs to their model and the reproducibility assumption of knee and hip motion kinematics from foot data for all movement patterns and subjects was the main restriction to their results. Our results, on the other hand, showed a superior accuracy in the estimation of trunk posture for both EKF and UKF optimal estimation techniques with the error values of 0.68 (0.11) deg and 1.16 (0.17) deg, respectively. In addition, our method is expandable to other gait conditions, including 3D movements, without any restriction on the motion patterns. Furthermore, the intersubject estimation of hip and trunk kinematics using EKF shows the reproducibility of the results for different body physical characteristics.

The proposed method of kinematics estimation for different body locations has many applications beyond fatigue assessment including in bioengineering, rehabilitaion, aging, and athletics. The need for body kinematics estimation is essential for any application that involves the analysis of stability and mobility of the human body. To be specific, the effectiveness of rehabilitation protocols are assessed for abnormal posture and movement diagnosis by the quantification of daily

physical activity after treatment [51]–[53]. In sport sciences, the lower body elastic energy capacity is evaluated by performance analysis in jump tasks using kinematic variables [54]. The traditional motion capture systems provide accurate measurement, however, the lack of portability is the limitation of such systems in capturing the body movements in a natural setting rather than a controlled laboratory environment. In addition, the optimality of the sensors in terms of the number and weight of the sensing units is another important criteria for making the system acceptable for the potential users [50]. In the proposed method, we have minimized the number of IMUs by employing only one sensor placed at the ankle that can be used for estimating the desired kinematics in any other body locations. Additionally, our method is able to estimate these metrics in a highly accurate manner as presented in the Results section with the novel approach of using Fourier series for the modeling of human walking instead of traditional biomechanical models, which significantly reduces the computational costs. The application of the present estimation method is intended to address the major challenges in the field of human motion analysis. To the best of our knowledge in this field, the use of EKF and UKF to estimate the body kinematics from a sensor in a specific location has not been studied.

V. Conclusion

This study provides an estimation technique for hip acceleration and trunk posture using optimal estimation algorithms along with a heuristically modified model using Fourier series from the data of a single IMU attached to the ankle that was originally limited to level ground gait. The Kalman filters generally require measurement data, although inaccurate, from the target locations. However, these limitations can be overcome by utilizing more simple and inexpensive sensors and the Kalman filter will perfectly make up the sensor errors. In addition, by tuning the Fourier series coefficients for any other specific activity (e.g. walking up/down the stairs, running, etc.), this method can also be applied to them likewise to the other metrics (e.g. velocity or jerk, etc.) and body locations (e.g. lower or upper extremities, etc.) for the purposes of human gait analysis, body fatigue detection, and other biomechanical/occupational safety applications.

References

[1] C. J. van Andel, N. Wolterbeek, C. A. Doorenbosch, D. H. Veeger, and J. Harlaar, "Complete 3d kinematics of upper extremity functional tasks," *Gait posture*, vol. 27, no. 1, pp. 120–127, 2008.

[2] A. Fern'ndez-Baena, A. Susiín, and X. Lligadas, "Biomechanical validation of upper-body and lower-body joint movements of Kinect motion capture data for rehabilitation treatments," in *Proc. IEEE 4th Int. Conf. Intell. Netw. Collaborative Syst. (INCoS)*, Sep. 2012, pp. 656–661.

[3] C. Frigo, R. Carabalona, M. D. Mura, and S. Negrini, "The upper body segmental movements during walking by young females," *Clin. Biomech.*, vol. 18, no. 5, pp. 419–425, 2003.

[4] J. Romkes, W. Peeters, A. M. Oosterom, S. Molenaar, I. Bakels, and R. Brunner, "Evaluating upper body movements during gait in healthy children and children with diplegic cerebral palsy," *J. Pediatric Orthopaedics B*, vol. 16, no. 3, pp. 175–180, 2007.

[5] M. Wisse, A. L. Schwab, and F. C. van der Helm, "Passive dynamic walking model with upper body," *Robotica*, vol. 22, no. 6, pp. 681–688, 2004.

[6] J. B. Dingwell and L. C. Marin, "Kinematic variability and local dynamic stability of upper body motions when walking at different speeds," *J. Biomech.*, vol. 39, no. 3, pp. 444–452, 2006.

[7] P. Simeonov, H. Hsiao, J. Powers, D. Ammons, T. Kau, and A. Amendola, "Postural stability effects of random vibration at the feet of construction workers in simulated elevation," *Appl. Ergonom.*, vol. 42, no. 5, pp. 672–681, 2011.

[8] G. P. Szeto, L. Straker, and S. Raine, "A field comparison of neck and shoulder postures in symptomatic and asymptomatic office workers," *Appl. Ergonom.*, vol. 33, no. 1, pp. 75–84, 2002.

[9] S. J. Ray and J. Teizer, "Real-time construction worker posture analysis for ergonomics training," *Adv. Eng. Inf.*, vol. 26, no. 2, pp. 439–455, 2012.

[10] T. Cheng and J. Teizer, "Real-time resource location data collection and visualization technology for construction safety and activity monitoring applications," *Autom. Construction*, vol. 34, pp. 3–15, Sep. 2013.

[11] M. Sallinen, E. Strömmer, and A. Ylisaukko-oja, "Application scenario for NFC: Mobile tool for industrial worker," in *Proc. IEEE 2nd Int. Conf. Sensor Technol. Appl., SENSORCOMM*, Aug. 2008, pp. 586–591.

[12] J. Yang, O. Arif, P. A. Vela, J. Teizer, and Z. Shi, "Tracking multiple workers on construction sites using video cameras," *Adv. Eng. Inf.*, vol. 24, no. 4, pp. 428–434, 2010.

[13] M. N. Nyan, F. E. Tay, and E. Murugasu, "A wearable system for pre-impact fall detection," *J. Biomech.*, vol. 41, no. 16, pp. 3475–3481, 2008.

[14] M. C. Schall, N. B. Fethke, and H. Chen, "Evaluation of four sensor locations for physical activity assessment," *Appl. Ergonom.*, vol. 53, pp. 103–109, 2016.

[15] S. Kim and M. A. Nussbaum, "Performance evaluation of a wearable inertial motion capture system for capturing physical exposures during manual material handling tasks," *Ergonomics*, vol. 56, no. 2, pp. 314–326, 2013.

[16] A. Baghdadi, F. M. Megahed, E. T. Esfahani, and L. A. Cavuoto, "A machine learning approach to detect changes in gait parameters following a fatiguing occupational task," *Ergonomics*, pp. 1–14, Mar. 2018. [Online]. Available: https://doi.org/10.1080/00140139.2018.1442936, doi: 10.1080/00140139.2018.1442936.

[17] A. M. Nardolillo, A. Baghdadi, and L. A. Cavuoto, "Heart rate variability during a simulated assembly task; influence of age and gender," in *Proc. Human Factors Ergonom. Soc. Annu. Meeting*, 2017, vol. 61. no. 1, pp. 1853–1857.

[18] H. Dejnabadi, B. M. Jolles, E. Casanova, P. Fua, and K. Aminian, "Estimation and visualization of sagittal kinematics of lower limbs orientation using body-fixed sensors," *IEEE Trans. Biomed. Eng.*, vol. 53, no. 7, pp. 1385–1393, Jul. 2006.

[19] V. Bonnet, C. Mazzàï¿½, P. Fraisse, and A. Cappozzo, "Real-time estimate of body kinematics during a planar squat task using a single inertial measurement unit," *IEEE Trans. Biomed. Eng.*, vol. 60, no. 7, pp. 1920–1926, Jul. 2013.

[20] W. Zijlstra and A. L. Hof, "Assessment of spatio-temporal gait parameters from trunk accelerations during human walking," *Gait Posture*, vol. 18, no. 2, pp. 1–10, Oct. 2003.

[21] S. Leteneur, C. Gillet, H. Sadeghi, P. Allard, and F. Barbier, "Effect of trunk inclination on lower limb joint and lumbar moments in able men during the stance phase of gait," *Clin. Biomech.*, vol. 24, no. 2, pp. 190–195, Feb. 2009.

[22] W. S. Marras, K. G. Davis, B. C. Kirking, and K. P. Granata, "Spine loading and trunk kinematics during team lifting," *Ergonomics*, vol. 42, no. 10, pp. 1258–1273, 1999.

[23] Z. S. Maman, A. Baghdadi, F. Megahed, and L. Cavuoto, "Monitoring and change point estimation of normal (in-control) and fatigued (out-of-control) state in workers," in *Proc. ASME Int. Design Eng. Tech. Conf. Comput. Inf. Eng. Conf.*, New York, NY, USA, 2016, p. V003T11A011.

[24] Z. S. Maman, M. A. A. Yazdi, L. A. Cavuoto, and F. M. Megahed, "A data-driven approach to modeling physical fatigue in the workplace using wearable sensors," *Appl. Ergonom.*, vol. 65, pp. 515–529, Nov. 2017.

[25] G. Rab, K. Petuskey, and A. Bagley, "A method for determination of upper extremity kinematics," *Gait posture*, vol. 15, no. 2, pp. 113–119, 2002.

[26] J. L. Crassidis and J. L. Junkins, *Optimization Estimation of Dynamic System*. Boca Raton, Florida, USA: CRC Press, 2011.

[27] M. St-Pierre and D. Gingras, "Comparison between the unscented kalman filter and the extended Kalman filter for the position estimation module of an integrated navigation information system," in *Proc. IEEE Int. Vehicles Symp.*, Jun. 2004, pp. 831–835.

[28] S. Patel *et al.*, "Monitoring motor fluctuations in patients with Parkinson's disease using wearable sensors," *IEEE Trans. Inf. Technol. Biomed.*, vol. 13, no. 6, pp. 864–873, Nov. 2009.
[29] B. R. Chen *et al.*, "A Web-based system for home monitoring of patients with parkinson's disease using wearable sensors," *IEEE Trans. Biomed. Eng.*, vol. 58, no. 3, pp. 831–836, Mar. 2011.
[30] B. R. Greene, D. McGrath, T. G. Foran, E. P. Doheny, and B. Caulfield, "Body-worn sensor based surrogates of minimum ground clearance in elderly fallers and controls," in *Proc. IEEE Annu. Int. Conf. Eng. Med. Biol. Soc., EMBC*, Aug. 2011, pp. 6499–6502.
[31] P. Vergallo, A. Lay-Ekuakille, F. Angelillo, I. Gallo, and A. Trabacca, "Accuracy improvement in gait analysis measurements: Kinematic modeling," in *Proc. IEEE Int. Instrum. Meas. Technol. Conf. (IMTC)*, May 2015, pp. 1987–1990.
[32] O. Costilla-Reyes, P. Scully, and K. B. Ozanyan, "Temporal pattern recognition in gait activities recorded with a footprint imaging sensor system," *IEEE Sensors J.*, vol. 16, no. 24, pp. 8815–8822, Dec. 2016.
[33] D. Gafurov, "A survey of biometric gait recognition: Approaches, security and challenges," in *Proc. Annu. Norwegian Comput. Sci. Conf.*, Nov. 2007, pp. 19–21.
[34] P. Rashidi and A. Mihailidis, "A survey on ambient-assisted living tools for older adults," *IEEE J. Biomed. Health Inform.*, vol. 17, no. 3, pp. 579–590, May 2013.
[35] D. Kim, A. Behbahani, R. M'closkey, P. Stupar, and J. Denatale, "Wafer-scale etch process for precision frequency tuning of MEMS gyros," in *Proc. IEEE Int. Symp. Inertial Sensors Syst. (ISISS)*, Mar. 2015, pp. 1–2.
[36] X. Yun and E. R. Bachmann, "Design, implementation, and experimental results of a quaternion-based Kalman filter for human body motion tracking," *IEEE Trans. Robot.*, vol. 22, no. 6, pp. 1216–1227, Dec. 2006.
[37] L. Ren, R. K. Jones, and D. Howard, "Predictive modelling of human walking over a complete gait cycle," *J. Biomech.*, vol. 40, no. 7, pp. 1567–1574, 2007.
[38] J. M. del Rincon, D. Makris, C. O. Urunuela, and J.-C. Nebel, "Tracking human position and lower body parts using Kalman and particle filters constrained by human biomechanics," *IEEE Trans. Syst., Man, Cybern. B, Cybern.*, vol. 41, no. 1, pp. 26–37, Feb. 2011.
[39] X. Yun, C. Aparicio, E. R. Bachmann, and R. B. McGhee, "Implementation and experimental results of a quaternion-based Kalman filter for human body motion tracking," in *Proc. IEEE Int. Conf. Robot. Autom.*, Apr. 2005, pp. 317–322.
[40] S. J. Julier, J. K. Uhlmann, and H. F. Durrant-Whyte, "A new approach for filtering nonlinear systems," in *Proc. Amer. Control Conf.*, vol. 3, Jun. 1995, pp. 1628–1632.
[41] J. J. LaViola, "A comparison of unscented and extended Kalman filtering for estimating quaternion motion," in *Proc. Amer. Control Conf.*, vol. 3, Jun. 2003, pp. 2435–2440.
[42] E. A. Wan and R. van der Merwe, "The unscented Kalman filter for nonlinear estimation," in *Proc. IEEE Adapt. Syst. Signal Process., Commun., Control Symp. (ASSPCC)*. Oct. 2000, pp. 153–158.
[43] S. J. Julier and J. K. Uhlmann, "A new extension of the Kalman filter to nonlinear systems," in *Proc. Int. Symp. Aerosp./Defense Sens., Simulation Controls*, Orlando, FL, USA, vol. 3, no. 26, 1997, pp. 182–193.
[44] F. Gustafsson and G. Hendeby, "Some relations between extended and unscented Kalman filters," *IEEE Trans. Signal Process.*, vol. 60, no. 2, pp. 545–555, Feb. 2012.
[45] L. Perea, J. How, L. Breger, and P. Elosegui, "Nonlinearity in sensor fusion: Divergence issues in EKF, modified truncated SOF, and UKF," in *Proc. AIAA Guid., Navigat. Control Conf. Exhib.*, 2007, p. 6514.
[46] N. Shafii, A. Khorsandian, A. Abdolmaleki, and B. Jozi, "An optimized gait generator based on Fourier series towards fast and robust biped locomotion involving arms swing," in *Proc. IEEE Int. Conf. Autom. Logistics (ICAL)*, Aug. 2009, pp. 2018–2023.
[47] A. Baghdadi, Z. S. Maman, L. Lu, L. A. Cavuoto, and F. M. Megahed, "Effects of task type, task duration, and age on body kinematics and subjective fatigue," in *Proc. Human Factors Ergonom. Soc. Annu. Meeting*, 2017, vol. 61. no. 1, p. 1040.
[48] P. Parijat and T. E. Lockhart, "Effects of lower extremity muscle fatigue on the outcomes of slip-induced falls," *Ergonomics*, vol. 51, no. 12, pp. 1873–1884, 2008.
[49] K. Yoshino, T. Motoshige, T. Araki, and K. Matsuoka, "Effect of prolonged free-walking fatigue on gait and physiological rhythm," *J. Biomech.*, vol. 37, no. 8, pp. 1271–1280, 2004.
[50] A. Findlow, J. Goulermas, C. Nester, D. Howard, and L. Kenney, "Predicting lower limb joint kinematics using wearable motion sensors," *Gait Posture*, vol. 28, no. 1, pp. 120–126, 2008.
[51] W. Y. Wong, M. S. Wong, and K. H. Lo, "Clinical applications of sensors for human posture and movement analysis: A review," *Prosthetics Orthotics Int.*, vol. 31, no. 1, pp. 62–75, 2007.
[52] B. Najafi, K. Aminian, A. Paraschiv-Ionescu, F. Loew, C. J. Bula, and P. Robert, "Ambulatory system for human motion analysis using a kinematic sensor: Monitoring of daily physical activity in the elderly," *IEEE Trans. Biomed. Eng.*, vol. 50, no. 6, pp. 711–723, Jun. 2003.
[53] M. Ghobadi and E. T. Esfahani, "A robust automatic gait monitoring approach using a single imu for home-based applications," *J. Mech. Med. Biol.*, vol. 17, no. 5, p. 1750077, 2017.
[54] K. Aminian and B. Najafi, "Capturing human motion using body-fixed sensors: Outdoor measurement and clinical applications," *Comput. Animation Virtual Worlds*, vol. 15, no. 2, pp. 79–94, 2004.

Amir Baghdadi received the B.Sc. degree from the Sharif University of Technology, Tehran, Iran, in 2014, and the M.Sc. degree in mechanical engineering from the University at Buffalo, State University of New York, NY, USA, in 2017, where he is currently pursuing the Ph.D. degree in mechanical engineering. He currently holds a Research Assistant position at the Department of Industrial and Systems Engineering, University at Buffalo. His research interests include the intersection of sensor fusion, data science, computer vision, and human factors. He was an Adjunct Faculty and an Instructor at The State University of New York College, Buffalo, and a Teaching Fellow with the Department of Mechanical and Aerospace Engineering, University at Buffalo. He is also a Research Scholar with Roswell Park Cancer Institute, Buffalo, NY, USA, where he has utilized computer vision methods for the first time to model automated assessment of surgical performance during robot-assisted surgery. He has received awards and fellowships for academic and entrepreneurship achievements including the Best Paper Award in Silent Hoist and Crane Company Materials Handling Graduate Paper Competition and the Student Entrepreneur Fellowship from the School of Management, University at Buffalo.

Lora A. Cavuoto received the M.S. degree in occupational ergonomics and safety from the University of Miami, Coral Gables, FL, USA, in 2008, and the M.S. and Ph.D. degrees in industrial and systems engineering from Virginia Tech, Blacksburg, VA, USA, in 2009 and 2012, respectively. She is currently an Assistant Professor with the Department of Industrial and Systems Engineering, University at Buffalo, Buffalo, NY, USA. She is currently the Director of the Ergonomics and Biomechanics Laboratory, University at Buffalo. Her current research interests include quantifying physical exposures and physiological responses in the workplace to identify indicators of fatigue development, to understand and model the effects of health conditions, particularly obesity and aging, on physical capacity, specifically strength, fatigue, and motor performance. She is currently an Associate Editor of *Human Factors and Ergonomics in Manufacturing and Service Industries* and serves on the Editorial Board of *Applied Ergonomics*.

John L. Crassidis received the B.S., M.S., and Ph.D. degrees from The State University of New York, Buffalo, Amherst, NY, USA, in 1989, 1991, and 1993, respectively, all in mechanical engineering. He was with the Catholic University of America and Texas A&M University. He is currently a CUBRC Professor of Space Situational Awareness with the Department of Mechanical and Aerospace Engineering. He was a Post-Doctoral Fellow with NASA's Goddard Space Flight Center. He is currently a Fellow of the American Institute of Aeronautics and Astronautics and the American Astronautical Society. He has received the AIAA Mechanics and Control of Flight Award, the AIAA/Society of Automotive Engineers J. Leland Atwood Award, the SAE Ralph R. Teetor Educational Award, and the AIAA Sustained Service Award.